Published in final edited form as:
Cancer Res. 2007 October 15; 67(20): 10047–10057. doi:10.1158/0008-5472.CAN-07-0523.

Cancer Immunotherapy Using Irradiated Tumor Cells Secreting Heat Shock Protein 70

Chih-Long Chang[1,5], **Ya-Chea Tsai**[1], **Liangmei He**[1], **T.-C. Wu**[1,2,3,4], and **Chien-Fu Hung**[1]

[1]Department of Pathology, Johns Hopkins Medical Institutions, Baltimore, Maryland [2]Departments of Obstetrics and Gynecology, Johns Hopkins Medical Institutions, Baltimore, Maryland [3]Department of Molecular Microbiology and Immunology, Johns Hopkins Medical Institutions, Baltimore, Maryland [4]Department of Oncology, Johns Hopkins Medical Institutions, Baltimore, Maryland [5]Department of Obstetrics and Gynecology, Mackay Memorial Hospital, Taipei, Taiwan

Abstract

Ovarian cancer is responsible for the highest mortality rate among patients with gynecologic malignancies. Therefore, there is an emerging need for innovative therapies for the control of advanced ovarian cancer. Immunotherapy has emerged as a potentially plausible approach for the control of ovarian cancer. In the current study, we have generated heat shock protein 70 (Hsp70)-secreting murine ovarian cancer cells that express luciferase (MOSEC/luc). Hsp70 has been shown to target and concentrate antigenic peptides in dendritic cells and is also able to activate dendritic cells. We characterized the antigen-specific immune response and the antitumor effect of the MOSEC/luc cells expressing Hsp70 using noninvasive luminescence images to measure the amount of ovarian tumors in the peritoneal cavity of mice. We found that mice challenged with MOSEC/luc cells expressing Hsp70 generate significant antigen-specific $CD8^+$ T-cell immune responses. Furthermore, we also found that mice vaccinated with irradiated MOSEC/luc cells expressing Hsp70 generate significant therapeutic effect against MOSEC/luc cells. In addition, we have shown that $CD8^+$, natural killer, and $CD4^+$ cells are important for protective antitumor effect generated by irradiated tumor cell–based vaccines expressing Hsp70. Moreover, we also found that CD40 receptor is most important, followed by Toll-like receptor 4 receptor, for inhibiting *in vivo* tumor growth of the viable MOSEC/luc expressing Hsp70. Thus, the use of Hsp70-secreting ovarian tumor cells represents a potentially effective therapy for the control of lethal ovarian cancer.

Introduction

There is an emerging need for innovative therapies for the control of advanced ovarian cancer. Ovarian cancer is responsible for the highest mortality rate among patients with gynecologic malignancies. Metastatic ovarian cancer is extremely difficult to cure and accounts for ~20% of total cancer mortalities among women. Current efforts to reduce this mortality rate, including improvements in early detection and treatment, have been relatively unsuccessful. Existing standard therapies for advanced disease, such as primary cytoreductive surgery followed by chemotherapy, rarely result in long-term benefits for

Requests for reprints: Chien-Fu Hung, Departments of Pathology and Oncology, The Johns Hopkins University School of Medicine, CRB II Room 307, 1550 Orleans Street, Baltimore, MD 21231. Phone: 410-614-3899; Fax: 443-287-4295; chung2@jhmi.edu..

Note: Supplementary data for this article are available at Cancer Research Online (http://cancerres.aacrjournals.org/).

patients with locally advanced and metastatic disease (1–3). Thus, identification of an alternative approach to control ovarian cancer represents an urgent concern.

Immunotherapy has emerged as a potentially plausible approach for the control of ovarian cancer. The ideal cancer therapy should have the potency to eradicate systemic tumors at multiple sites in the body as well as the specificity to discriminate between malignant and normal cells. In both of these respects, the immune system is an attractive candidate. The immune system is composed of several effector cells that are capable of killing target cells. B and T cells can generate tumor-specific responses because they have a vast array of clonally distributed antigen receptors, which can recognize antigens expressed only by tumors. It is well established that T cells recognize peptide fragments of cellular proteins bound to MHC molecules on the surface of cells, and any cellular protein (including those from which tumor antigens derive) can be presented to T cells in this way. However, few therapies that augment the host immune response have been applied to patients with ovarian cancer. One of the novel therapeutic approaches is the use of tumor cells secreting heat shock proteins (Hsp).

Hsps isolated from tumor extracts have been shown to generate tumor-specific T-cell responses and antitumor effects (4, 5). We have shown that linkage of Hsp70 to a model tumor antigen, human papillomavirus (HPV) E7, elicits strong antitumor immunity against tumors expressing HPV E7 (6). Secreted Hsps, such as gp96, gp170, and Hsp70, bound with antigenic peptides are targeted to and concentrated in dendritic cells. Furthermore, Hsps are able to activate dendritic cells (5, 7, 8). An advantage to using the secreted form of Hsp is there is a consistent availability of Hsp70 rather than only after apoptosis of Hsp70-containing cells. All of these features enhance the priming of antigen-specific T cells and lead to a strong antitumor effect. Recently, tumor cell–based vaccines engineered to secrete Hsp70 have been shown to effectively control tumor growth (9–11). We (12) and others (13) have also shown that DNA vaccines encoding secreted Hsp70 linked with HPV E7 could generate potent immune responses against E7 and a stronger antitumor effect against E7-expressing TC-1 tumor cells. Thus, tumor cell–based vaccines using Hsps could potentially play an important role in ovarian cancer immunotherapy.

One of the major limitations to ovarian cancer immunotherapy is the difficulty of generating ovarian cancer mouse models. Without suitable ovarian cancer models in immune intact mice, it will be difficult to test new therapies for ovarian cancers. Mouse ovarian surface epithelial cells (MOSEC) from immune intact mice were developed *in vitro* by Roby et al. (14). The MOSEC ovarian cancer model was created by isolating ovarian surface epithelial cells from virgin, mature mice and culturing *in vitro* for >20 passages. I.p. injection of late-passage MOSEC cells into immune intact mice resulted in the formation of ascitic fluid and multiple tumor implants in the peritoneal cavity that resembled those seen in stage III and IV ovarian cancer patients. Another significant challenge in the field of ovarian cancer immunotherapy is the difficulty in assessing tumor load in the peritoneal cavity. Recently, we (15) and others (16) have developed noninvasive bioluminescence images to measure the amount of ovarian tumors in the peritoneal cavity of mice. We found that luciferase activities correlated with the tumor loads of ovarian cancer injected in the peritoneal cavity of mice. Furthermore, the luminescence activity correlated inversely with mouse survival rate. Thus, the noninvasive bioluminescence imaging system represents a suitable method to assess the ovarian cancer tumor load.

In the current study, we have generated Hsp70-secreting murine ovarian cancer cells (MOSEC) that express luciferase. We found that mice challenged with MOSEC-luciferase (MOSEC/luc) cells expressing Hsp70 generate significant antigen-specific $CD8^+$ T-cell immune response. Furthermore, we also found that mice vaccinated with irradiated MOSEC/

luc cells expressing Hsp70 generate significant therapeutic effect against MOSEC/luc cells. In addition, we have shown that $CD8^+$, natural killer (NK), and $CD4^+$ cells are important for protective antitumor effect generated by irradiated tumor cell–based vaccines expressing Hsp70. We also found that CD40 receptor is most important, followed by Toll-like receptor (TLR) 4 receptor, for inhibiting *in vivo* tumor growth of the viable MOSEC/luc expressing Hsp70. Thus, the use of Hsp70-secreting ovarian tumor cells represents a potentially novel therapy that may generate an effective therapeutic approach for the control of lethal ovarian cancer. The clinical implication of the current study is discussed.

Materials and Methods

Mice

Female C57BL/6 mice were acquired from the National Cancer Institute. Female $CD40^{-/-}$ (B6.129P2-*CD40*^{tm1Kik}/J) mice, $TLR4^{lps\text{-}del}$ (C57BL/10ScNJ) mice, and $TLR2^{-/-}$ ($TLR2^{tm1Kir}$/$TLR2^{tm1Kir}$, B6.129-*TLR2*^{tm1Kir}/J) mice were purchased from The Jackson Laboratory. All animals were maintained under specific pathogen-free conditions, and all procedures were done according to approved protocols and in accordance with recommendations for the proper use and care of laboratory animals.

Plasmid DNA constructs and DNA preparation

For generation of retroviral plasmids encoding murine secretory Hsp70-T2A peptide (sHsp70)-green fluorescent protein (GFP) and the control T2A peptide-GFP, murine Hsp70 was first cloned into pSecTag2 B (Invitrogen) by PCR cloning using the forward primer 5′-CCCAAGCTTATGGCCAAGAACACGGCGAT-3′ containing a *Hin*dIII enzyme site and the backward primer 5′-CGGGATCCATCCACCTCCTCGATGGTGG-3′ containing a *Bam*HI site. The sequences between *Nhe*I and *Bam*HI, which contains one murine immunoglobulin κ-chain signal peptide fused with Hsp70, were subcloned into the *Not*I (blunted) and *Bam*HI sites of a retroviral vector pMSCV-FLAG. Two complementary oligonucleotides encoding *Thosea asigna* virus 2A peptide EGRGSLLTCGDVEENPGP (17) containing *Bam*HI site on one and *Eco*RI site on the other were synthesized, annealed, and cloned into the corresponding sites of pMSCV-FLAG. *Enhanced GFP* (*EGFP*) gene was inserted between *Eco*RI and *Xho*I. The control plasmid pMSCV-T2A-GFP consists of the same arrangements of genes but devoid of sHsp70. A retroviral construct pLuci-thy1.1 expressing both luciferase and thy1.1 was reported before (15). The amplified luciferase cDNA was inserted into the *Bgl*II and *Hpa*I sites of the bicistronic vector pMIG-thy1.1. Both luciferase and thy1.1 cDNA are under the control of a single promoter element and separated by internal ribosomal entry site. All of the constructs were verified by restriction analysis and DNA sequencing using ABI 3730 DNA Analyzer by Johns Hopkins DNA analysis facility.

Cell lines

The MOSEC and TC-1 cell lines were generated as shown previously (14, 18). The MOSEC cell line was originally derived from mouse ovarian surface epithelial cells (14). TC-1 cell line was generated by *in vitro* culture of primary lung epithelial cells and transduction with HPV-16 E6 and E7 transformative genes, which immortalized the cells, as well as the *c*-Ha-ras oncogene (18). MOSEC/luc or TC-1-luciferase (TC-1/luc) cells were generated as described previously (19). For stable expression of sHsp70-GFP and GFP on these two cell lines, pMSCV-FLAG/sHsp70-T2A-GFP or GFP was transfected into Phoenix packaging cell line using LipofectAMINE (Invitrogen) and the virion-containing supernatant was collected 48 h after transfection. The supernatant was then filtered through a 0.45-mm cellulose acetate syringe filter (Nalgene) and used to infect MOSEC/luc cells in the presence of 8 mg/mL polybrene (Sigma). Transduced cells were isolated using preparative flow

cytometry of stained cells with GFP signal sorting. The growth rate of MOSEC/luc (or TC-1/luc)/Hsp70-GFP cells was comparable with those of MOSEC/luc (or TC-1/luc)/GFP cells (data not shown).

Western blot

To detect Hsp70 protein expression in the culture medium and cells, 1×10^5 MOSEC/luc/sHsp70-T2A-GFP and MOSEC/luc/GFP cells were seeded in six-well plate. Forty-eight hours after seeding the cells, medium from culture was collected and cells were lysed with protein extraction reagent (Pierce). Equal amounts of proteins (10 μg) or medium (30 μL) were loaded and separated by SDS-PAGE using a 10% polyacrylamide gel. The gels were electroblotted to a polyvinylidene difluoride membrane (Bio-Rad Laboratories). Blots were blocked with PBS/0.05%, Tween 20 (TTBS) containing 5% nonfat milk for 2 h at room temperature. Membranes were probed with rabbit anti-Hsp70 antibody (StressGen) for 1 h, washed four times with TTBS, and then incubated with sheep anti-mouse IgG conjugated to horseradish peroxidase (Amersham) at 1:1,000 dilution in TTBS containing 5% nonfat milk. Membranes were washed four times with TTBS and visualized under ChemiDoc XRS chemiluminescent detection system (Bio-Rad Laboratories).

Tumorigenesis assay

Naive C57BL/6 mice were challenged i.p. with 1×10^6 live TC-1/luc/sHsp70-GFP and TC-1/luc/GFP or 1×10^6 MOSEC/luc/sHsp70-GFP and MOSEC/luc/GFP. $CD40^{-/-}$, $TLR4^{lps\text{-}del}$, and $TLR2^{-/-}$ mice were challenged with 1×10^6 live MOSEC/luc/sHsp-GFP and MOSEC/luc/GFP cells. Detection of luminescence activity indicating relative tumor loading was done by Xenogeny IVIS 200 Imaging System on a weekly basis.

Tumor protection assay

Naive C57BL/6 mice were i.p. injected with 1×10^6 live or irradiated MOSEC/luc/GFP cells and MOSEC/luc/sHsp70-GFP cells. The irradiated MOSEC/luc/GFP or MOSEC/luc/sHsp70-GFP tumor cells were prepared using an irradiation dosage of 90,000 cGy/10 min. Luciferase activity was checked 2 weeks later. For those mice in which tumor luminescent activities have declined by 2 weeks (except live MOSEC/luc/GFP group), 1×10^6 MOSEC/luc cells were used to i.p. challenge again 2 weeks after vaccination. Differences in the luminescence activity of tumor growth were monitored once weekly.

Tumor treatment

C57BL/6 mice were i.p. injected with 1×10^6 MOSEC/luc cells. After 5 days, mice were treated with irradiated 1×10^6 MOSEC/luc/GFP or MOSEC/luc/sHsp70-GFP cells. Differences in the luminescence activity of tumor growth were monitored once weekly.

Depletion of lymphocyte subsets *in vivo*

Those mice vaccinated with irradiated 1×10^6 MOSEC/luc/sHsp-GFP or MOSEC/luc/GFP cells were injected i.p. with blocking antibody using a protocol similar to one described previously (20). Mice were injected with 100 Ag of purified rat monoclonal antibody (mAb) GK1.5 (anti-CD4), 2.43 (anti-CD8), and PK136 (anti-NK1.1). Depletion was started 1 week after cell-based vaccination and continued every other day for the first week and then once every week. Depletion was assessed 1 day after the third administration of antibodies and 1 day after the fourth administration of antibodies by flow cytometry analysis of spleen cells stained with 2.43, GK1.5, or PK136. We found that >90% depletion of CD8, CD4, or NK cells was achieved. These mice were challenged with MOSEC/luc tumor cells 2 weeks after vaccination. Depletion was maintained by continuing the antibody injections weekly for the

duration of the tumor imaging follow-up. Differences in the luminescence activity of tumor growth were monitored once weekly.

Intracellular cytokine staining and flow cytometry analysis

Mice were vaccinated with 1×10^6 irradiated MOSEC/luc/Hsp70-GFP or MOSEC/luc/GFP or 1×10^6 irradiated TC-1/luc/Hsp70-GFP or TC-1/luc/GFP cells twice at 1-week interval. Splenocytes were harvested from mice 1 week after the last vaccination. Pooled splenocytes (5×10^6) from each vaccination group were incubated for 7 days with 1 μg/mL murine mesothelin peptide (for MOSEC cell lines, amino acids 406–414; ref. 21) or with no peptide as control. For TC-1 cell lines, pooled splenocytes were stimulated with 1 μg/mL murine E7 peptide (amino acids 49–57; ref. 22) or no peptide overnight directly. Cell surface marker staining for CD8 and intracellular cytokine staining for IFN-γ as well as flow cytometry analysis were done under conditions described previously (20). Analysis was done on a Becton Dickinson FACScan with CellQuest software (Becton Dickinson Immunocytometry System). Each group was measured in triplicate and data were shown as mean ± SD in numerical bar.

Statistical analysis

All data expressed as mean ± SD are representative of at least two different experiments. Comparisons between individual data points were made using a Student's *t* test. Differences in survival between experimental groups were analyzed using the Kaplan-Meier approach. The statistical significance of group differences will be assessed using the log-rank test.

Results

Cells transduced with retrovirus encoding Hsp70-GFP express the secreted form of the mouse Hsp70 protein

We generated the retrovirus encoding sHsp70-T2A-GFP (referred to as Hsp70-GFP) or T2A-GFP (referred to as GFP). The GFP expression in cells allowed us to distinguish transfected cells from untransfected cells. Furthermore, T2A is a self-cleavage peptide from *T. asigna* virus that cleaves cotranslationally and allowed us to determine the effect of secreted Hsp70 (17). To characterize whether MOSEC/luc cells transduced with retrovirus encoding Hsp70-GFP or GFP express comparable levels of the gene encoded by the retrovirus, we did flow cytometry analysis for GFP expression. As shown in Fig. 1*A*, comparable levels of GFP expression were observed in both the MOSEC/luc cells transduced with Hsp70-GFP and MOSEC/luc cells transduced with GFP. To further determine if MOSEC/luc cells transduced with retrovirus encoding Hsp70-GFP led to secretion of the mouse Hsp70 protein in the culture medium, we did Western blot using the supernatant from cultured MOSEC/luc cells transduced with Hsp70-GFP or GFP. As shown in Fig. 1*B*, the supernatant of MOSEC/luc cells transduced with Hsp70-GFP contained a 70-kDa protein, consistent with the secreted form of mouse Hsp70 protein, as well as an ~100-kDa protein, which represents the uncleaved fusion protein of sHsp70 and EGFP. We also determined the total amount of secreted Hsp70 from irradiated MOSEC/luc/sHsp70-GFP cells in culture using the ELISA. Purified recombinant Hsp70 protein from bacteria was used to generate a standard curve. We found the concentration of Hsp70 from the supernatant of 1×10^6 of irradiated MOSEC/luc/sHsp70-GFP cells seeded on the culture dish for 24 h to be 74.36 ± 2.87 ng/mL. Because the whole amount of the supernatant is 2 mL, the total amount of Hsp70 protein secreted from 1×10^6 of irradiated MOSEC/luc/sHSp70-GFP cells in 24 h is 148.72 ng. Thus, our data indicate that MOSEC/luc cells transduced with Hsp70-GFP express the secreted form of Hsp70 protein.

Mice challenged with MOSEC/luc cells expressing Hsp70-GFP fail to develop tumor growth

We then tested the *in vivo* tumor growth in mice challenged with MOSEC/luc cells expressing Hsp70-GFP or GFP. The tumor growth of the challenged mice was characterized using bioluminescent imaging systems. As shown in Fig. 1*C*, the mice challenged with MOSEC/luc cells expressing Hsp70-GFP showed a significant reduction in luciferase activity over time. In contrast, the mice challenged with MOSEC/luc cells expressing GFP showed increased luciferase activity over time. The luciferase activity of the tumor-challenged mice was quantified in the form of bar graphs (Fig. 1*D*). Our data suggest that viable MOSEC/luc cells expressing Hsp70-GFP failed to grow in tumor-challenged mice. We also characterized the *in vitro* proliferation rate and *in vivo* growth rate in nude mice of MOSEC/luc cells expressing Hsp70-GFP and MOSEC/luc cells expressing GFP, and we found no significant difference in proliferation (data not shown). Thus, the fact that MOSEC/luc cells expressing Hsp70-GFP failed to grow in tumor-challenged mice is not due to differences in proliferation of MOSEC/luc cells expressing Hsp70-GFP and MOSEC/luc cells expressing GFP or to the toxicity of transfection of cells with GFP.

We also did an ELISA to determine the serum levels of secreted Hsp70 in vaccinated mice. Purified recombinant Hsp70 protein from bacteria was used to generate a standard curve. Mice were vaccinated with MOSEC/luc/sHsp70-GFP or MOSEC/luc/GFP (control) cells at doses of 1×10^6 or 2×10^7 cells per mouse. Sera from vaccinated mice were taken on× days 0, 3, and 7. We found that Hsp70 was only detectable after injection of MOSEC/luc/sHsp70-GFP cells at a dose of 2×10^7 cells per mouse on day 3 (see Supplementary Fig. S1). The concentration of the serum Hsp70 was determined to be 18.17 ± 4.3 ng/mL. Because Hsp70 is bound to scavenger receptors such as CD91 (23), which are commonly expressed in macrophages and other types of cells *in vivo*, the secreted Hsp70 may be easily absorbed from the serum, resulting in low serum levels. Thus, it is difficult to detect serum Hsp70 unless large amounts of MOSEC/luc/sHsp70-GFP cells were injected.

Mice previously challenged with MOSEC/luc cells expressing Hsp70-GFP generate long-term protective antitumor effects against MOSEC/luc and prolonged survival

To determine if the mice previously challenged with MOSEC/luc cells expressing Hsp70-GFP generate long-term antitumor effects against MOSEC/luc, we did an *in vivo* tumor protection experiment. The previously challenged mice were rechallenged i.p. with MOSEC/luc cells. Naive mice were also challenged with MOSEC/luc as a control. The tumor growth of the MOSEC/luc cells in challenged mice was monitored using bioluminescent imaging systems. As shown in Fig. 2A, the mice previously challenged with MOSEC/luc cells expressing Hsp70-GFP showed a significant reduction in luciferase activity over time. In contrast, the naive mice challenged with MOSEC/luc cells showed increased luciferase activity over time. The luciferase activity of the tumor-challenged mice was quantified in the form of bar graphs, as shown to the right. These data indicate that the mice previously challenged with MOSEC/luc cells expressing Hsp70-GFP generated long-term protective antitumor effects against MOSEC/luc cells. We further characterized the survival of tumor-challenged mice using the Kaplan-Meier survival analysis. As shown in Fig. 2*B*, prolonged survival was observed in mice previously challenged with MOSEC/luc cells expressing Hsp70-GFP compared with naive mice control. Taken together, our data suggest that mice previously challenged with MOSEC/luc cells expressing Hsp70-GFP generate a long-term protective antitumor effect and prolonged survival.

Mice immunized with irradiated MOSEC/luc cells expressing Hsp70-GFP show significant decrease in tumor load and prolonged survival

For clinical translation, it is important to use irradiated tumor cell–based vaccines instead of live tumor cell–based vaccines. We thus did an *in vivo* tumor protection experiment using

irradiated MOSEC/luc cells expressing Hsp70-GFP. C57BL/6 mice were immunized i.p. with 1×10^6 per mouse of irradiated MOSEC/luc cells expressing either Hsp70-GFP or GFP. The irradiated MOSEC/luc/GFP or MOSEC/luc/sHsp70-GFP tumor cells were prepared by using an irradiation dosage of 90,000 cGy/10 min. Two weeks later, the mice were challenged with MOSEC/luc cells. The tumor growth of the challenged mice was characterized using bioluminescent imaging systems. As shown in Fig. 2*C*, the mice immunized with irradiated MOSEC/luc expressing Hsp70-GFP showed a significant reduction in luciferase activity over time. In contrast, the mice immunized with irradiated MOSEC/luc cells expressing GFP showed increased luciferase activity over time. The luciferase activity was quantified in the form of bar graphs, as shown to the right. These data suggest that immunization with irradiated MOSEC/luc cells expressing Hsp70-GFP generates a protective antitumor effect. We characterized the survival of the tumor-challenged mice using Kaplan-Meier survival analysis. As shown in Fig. 2*D*, we observed prolonged survival in mice immunized with irradiated MOSEC/luc cells expressing Hsp70-GFP compared with mice immunized with irradiated MOSEC/luc cells expressing GFP. Taken together, our data suggest that immunization with irradiated MOSEC/luc cells expressing Hsp70-GFP generates a protective antitumor effect and prolongs survival.

Mice challenged with TC-1/luc cells expressing mouse Hsp70-GFP show slow development of tumor growth and longer survival

To determine whether the effect observed in mice immunized with MOSEC/luc tumor cells expressing Hsp70-GFP is applicable to other tumor models, we observed the tumor growth in the TC-1 tumor cell line. This is a highly potent tumor cell line and expresses highly specialized tumor antigens. The C57BL/6 mice were challenged with viable TC-1/luc cells expressing either Hsp70-GFP or GFP and were characterized using bioluminescent imaging systems. We observed a significant reduction in luciferase activity over time in the mice challenged with TC-1/luc cells expressing Hsp70-GFP. The luciferase activity was quantified in the form of bar graphs (see Supplementary Fig. S2). Thus, our data suggest that viable TC-1/luc cells expressing Hsp70-GFP showed slow tumor growth in challenged mice similar to what is observed in the case of MOSEC/luc cells expressing Hsp70-GFP. Furthermore, when mice were immunized with irradiated TC-1/luc cells expressing Hsp70-GFP, the vaccinated mice also generated potent protective antitumor effects (data not shown).

Mice vaccinated with irradiated tumor cells expressing Hsp70-GFP generate significantly high frequency of activated antigen-specific $CD8^+$ T cells

To determine the antigen-specific $CD8^+$ T-cell immune responses in mice vaccinated with irradiated tumor cells expressing Hsp70-GFP, we did flow cytometry analyses to determine the number of antigen-specific IFN-γ–secreting $CD8^+$ T cells using splenocytes from vaccinated mice. C57BL/6 mice were vaccinated i.p. with either TC-1/luc cells expressing Hsp70-GFP or GFP (Fig. 3*A* and *B*) or MOSEC/luc cells expressing Hsp70-GFP or GFP (Fig. 3*C* and *D*). Because the TC-1 has been shown to express HPV-16 E7 and MOSEC cells have been shown to express mesothelin, we focus on characterizing the E7 or mesothelin-specific $CD8^+$ T-cell immune response in mice vaccinated with irradiated TC-1 cells expressing Hsp70-GFP or irradiated MOSEC/luc cells expressing Hsp70-GFP, respectively. Splenocytes from vaccinated mice were stimulated with either E7- or mesothelin-specific peptides. The E7-specific antigenic peptide (amino acids 49–57; ref. 22) and the mesothelin-specific peptide (amino acids 406–414; ref. 21) have been characterized as a MHC class I–restricted $CD8^+$ T-cell epitope in C57BL/6 mice. Thus, these peptides allow us to characterize the E7- or mesothelin-specific immune response in vaccinated mice. As shown in Fig. 3*A* and *C*, significantly higher number of antigen-specific IFN-γ–secreting $CD8^+$ T cells was observed in mice vaccinated with irradiated tumor cells expressing

Hsp70-GFP compared with mice vaccinated with irradiated tumor cells expressing GFP. A graphical representation of the number of IFN-γ^+ $CD8^+$ T cells is depicted in Fig. 3*B* and *D*. Our data indicate that mice vaccinated with irradiated tumor cells expressing Hsp70-GFP are capable of generating a potent antigen-specific $CD8^+$ T-cell immune response.

$CD8^+$, NK, and $CD4^+$ cells are important for protective antitumor effect generated by irradiated tumor cell–based vaccines expressing Hsp70-GFP

To determine the major subset of lymphocytes important for the protective antitumor effect observed in mice vaccinated with irradiated MOSEC/luc cells expressing Hsp70-GFP, we did *in vivo* antibody depletion experiments using mAbs specific for $CD4^+$ T cells, $CD8^+$ T cells, or NK cells. C57BL/6 mice were vaccinated with irradiated MOSEC/luc expressing Hsp70-GFP. Mice vaccinated with irradiated MOSEC/luc cells expressing GFP without lymphocyte depletion were used as a control. Two weeks after vaccination, the mice were challenged with MOSEC/luc cells. Depletion was initiated 1 week before tumor challenge. Tumor growth was monitored using bioluminescent imaging systems. As shown in Fig. 4*A*, we observed the high luciferase activity in Hsp70-GFP–vaccinated mice depleted of $CD8^+$, NK, or $CD4^+$ cells compared with the vaccinated mice without depletion. A graphical representation of the luminescent activity data is depicted in Fig. 4*B*. Thus, our data suggest that the $CD8^+$, NK, and $CD4^+$ cells are important for protective antitumor immunity observed in mice vaccinated with irradiated MOSEC/luc cells expressing Hsp70-GFP.

Vaccination with irradiated MOSEC/luc cells expressing Hsp70-GFP generates a significant therapeutic antitumor effect and promotes long-term survival

To test the therapeutic effects of treatment with irradiated MOSEC/luc cells expressing Hsp70-GFP, we challenged C57BL/6 mice i.p. first with MOSEC/luc cells and then treated them 5 days later with irradiated MOSEC/luc cells expressing either Hsp70-GFP or GFP. Tumor growth in tumor-challenged mice was then monitored using bioluminescent imaging systems. As shown in Fig. 5*A*, we observed significant reduction in luciferase activity in mice treated with irradiated MOSEC/luc cells expressing Hsp70-GFP over time. In comparison, the tumor-challenged mice treated with irradiated MOSEC/luc cells expressing GFP showed an increase in luciferase activity over time. A graphical representation of the luciferase activity data is depicted in Fig. 5*B*. These data suggest that treatment with irradiated MOSEC/luc cells expressing Hsp70-GFP leads to significant therapeutic antitumor effect. We also characterized the survival of the treated mice using the Kaplan-Meier survival analysis. As shown in Fig. 5*C*, we observed prolonged survival in mice treated with irradiated MOSEC/luc cells expressing Hsp70-GFP compared with mice treated with irradiated MOSEC/luc cells expressing GFP. Thus, our data indicate that treatment with irradiated MOSEC/luc cells expressing Hsp70-GFP leads to significant therapeutic antitumor effect and prolonged survival.

CD40 and TLR4 receptors are important for inhibiting *in vivo* tumor growth of the viable MOSEC/luc expressing Hsp70-GFP

It has also been implicated that CD40, TLR2, and TLR4 (10, 24–29) can bind with Hsp70 and are important for Hsp70-mediated immune adjuvant effects. To determine if these molecules are important for inhibiting *in vivo* tumor growth of the viable MOSEC/luc expressing Hsp70-GFP, we tested the *in vivo* tumor growth in CD40, TLR2, or TLR4 knockout C57BL/6 mice. The mice were challenged with 1×10^6 per mouse of viable MOSEC/luc cells expressing Hsp70-GFP. Naive mice were included as a control. The tumor growth of the challenged mice was characterized using bioluminescent imaging systems and luciferase activity was quantified in the form of bar graphs. As shown in Fig. 6, the naive mice and TLR2 knockout mice challenged with MOSEC/luc cells expressing Hsp70-GFP showed a significant reduction in tumor growth (luciferase activity) over time. In contrast,

the CD40 knockout mice challenged with MOSEC/luc cells expressing GFP showed the most significant increase in tumor growth (luciferase activity) over time. The TLR4 knockout mice challenged with MOSEC/luc cells expressing GFP showed moderate increase in tumor growth (luminescent activity). Our data suggest that viable MOSEC/luc cells expressing Hsp70-GFP failed to grow in tumor-challenged naive and TLR2 knockout mice but did grow largely in CD40 and minimally in TLR4 knockout mice. Thus, CD40 is the most important protein, followed by TLR4, in the mechanism of the inhibiting tumors expressing Hsp70-GFP.

Discussion

In the current study, we have generated Hsp70-secreting murine ovarian cancer cells (MOSEC) that express luciferase. We found that mice challenged with MOSEC/luc cells expressing Hsp70-GFP generate significant mesothelin-specific $CD8^+$ T-cell immune responses and significant therapeutic effect against MOSEC/luc cells. Furthermore, the same approach is applicable to other tumor models, such as E7-expressing TC-1 tumor cell models. In addition, we have shown that the protective antitumor effect is mainly contributed to by $CD8^+$, NK, and $CD4^+$ cells. We also found that CD40 and TLR4 receptors are important for inhibiting *in vivo* tumor growth of the viable MOSEC/luc expressing Hsp70. We have shown that the use of the noninvasive bioluminescence imaging systems serves as great tool for characterizing the tumor load over time. Our observations serve as an important foundation for future clinical translation.

In this study, we observe significant enhancement of antigen-specific immune response in mice vaccinated with irradiated tumor cells secreting Hsp70. There are several properties of Hsp70 that may contribute to the generation of antigen-specific $CD8^+$ T-cell immune responses. For example, Hsp70 has been shown to bind with antigenic peptides and is capable of binding with CD91 receptor on antigen-presenting cells (23). Furthermore, Hsp has been shown to facilitate cross-presentation of bound antigenic peptide (30–32). Moreover, Hsp is capable of activating dendritic cells (33). Thus, a combination of these factors significantly contributes to the generation of antigen-specific immune responses generated by tumor cells secreting Hsp70.

In the current study, we observed that CD40 is most important for inhibiting tumor growth of MOSEC/luc cells expressing Hsp70-GFP. CD40 is an extracellular receptor for binding and uptake of Hsp70-peptide complexes (29). The binding of Hsp70-peptide complexes from tumor cells with CD40 may facilitate the cross-presentation of tumor-antigenic peptides by antigen-presenting cells. Furthermore, binding of Hsp70-peptide complexes to antigen-presenting cells that express CD40 may also lead to activation of dendritic cells, resulting in secretion of proinflammatory cytokines via p38/nuclear factor-κB signaling pathway (29). Thus, the CD40 molecule is crucial for the inhibition of the growth of tumor cells expressing Hsp70-GFP.

The newly created MOSEC/luc tumor model will serve as an important model for the characterization of tumor load and distribution in tumor-challenged mice using noninvasive bioluminescence imaging. Previous studies also validate the use of bioluminescence imaging system for quantitatively measuring tumor load *in vivo* (16, 34–36). We also characterized the tumor load by gross examination of the peritoneal cavity and found that the tumor volume correlates with the intensity of the luminescence imaging. Furthermore, the luminescence activity correlated well with mouse survival rate. Thus, the bioluminescence imaging used in this study represents a plausible noninvasive approach to measure tumor load and distribution in mice.

Supplementary Material

Refer to Web version on PubMed Central for supplementary material.

Acknowledgments

Grant support: Alliance for Cancer Gene Therapy, American Cancer Society, and NCDGG (1U19 CA113341-01).

The costs of publication of this article were defrayed in part by the payment of page charges. This article must therefore be hereby marked *advertisement* in accordance with 18 U.S.C. Section 1734 solely to indicate this fact.

We thank Dr. Richard Roden for helpful discussions and Archana Monie and Talia Hoory for the preparation of the manuscript.

References

1. Pfisterer J, Ledermann JA. Management of platinum-sensitive recurrent ovarian cancer. Semin Oncol. 2006; 33:S12–6. [PubMed: 16716798]
2. Bhoola S, Hoskins WJ. Diagnosis and management of epithelial ovarian cancer. Obstet Gynecol. 2006; 107:1399–410. [PubMed: 16738170]
3. Ozols RF. Systemic therapy for ovarian cancer: current status and new treatments. Semin Oncol. 2006; 33:S3–11. [PubMed: 16716797]
4. Tamura Y, Peng P, Liu K, Daou M, Srivastava PK. Immunotherapy of tumors with autologous tumor-derived heat shock protein preparations. Science. 1997; 278:117–20. [PubMed: 9311915]
5. Srivastava PK, Udono H, Blachere NE, Li Z. Heat shock proteins transfer peptides during antigen processing and CTL priming. Immunogenetics. 1994; 39:93–8. [PubMed: 8276462]
6. Chen C- H, Suh KW, Ji H, Choti MA, Pardoll DM, Wu T- C. Antigen-specific immunotherapy for HPV-16 E7-expressing tumors grown in liver. J Hepatology. 2000; 33:91–8.
7. Singh-Jasuja H, Hilf N, Scherer HU, et al. The heat shock protein gp96: a receptor-targeted cross-priming carrier and activator of dendritic cells. Cell Stress Chaperones. 2000; 5:462–70. [PubMed: 11189453]
8. Spee P, Neefjes J. TAP-translocated peptides specifically bind proteins in the endoplasmic reticulum, including gp96, protein disulfide isomerase and calreticulin. Eur J Immunol. 1997; 27:2441–9. [PubMed: 9341791]
9. Yamazaki K, Nguyen T, Podack ER. Cutting edge: tumor secreted heat shock-fusion protein elicits CD8 cells for rejection. J Immunol. 1999; 163:5178–82. [PubMed: 10553037]
10. Massa C, Guiducci C, Arioli I, Parenza M, Colombo MP, Melani C. Enhanced efficacy of tumor cell vaccines transfected with secretable hsp70. Cancer Res. 2004; 64:1502–8. [PubMed: 14973071]
11. Wang XY, Arnouk H, Chen X, Kazim L, Repasky EA, Subjeck JR. Extracellular targeting of endoplasmic reticulum chaperone glucose-regulated protein 170 enhances tumor immunity to a poorly immunogenic melanoma. J Immunol. 2006; 177:1543–51. [PubMed: 16849461]
12. Trimble C, Lin CT, Hung CF, et al. Comparison of the $CD8^+$ T cell responses and antitumor effects generated by DNA vaccine administered through gene gun, biojector, and syringe. Vaccine. 2003; 21:4036–42. [PubMed: 12922140]
13. Hauser H, Shen L, Gu QL, Krueger S, Chen SY. Secretory heat-shock protein as a dendritic cell-targeting molecule: a new strategy to enhance the potency of genetic vaccines. Gene Ther. 2004; 11:924–32. [PubMed: 15085173]
14. Roby KF, Taylor CC, Sweetwood JP, et al. Development of a syngeneic mouse model for events related to ovarian cancer. Carcinogenesis. 2000; 21:585–91. [PubMed: 10753190]
15. Hung CF, Tsai YC, He L, et al. Vaccinia virus preferentially infects and controls human and murine ovarian tumors in mice. Gene Ther. 2007; 14:20–9. [PubMed: 16915291]
16. Tseng JC, Levin B, Hurtado A, et al. Systemic tumor targeting and killing by Sindbis viral vectors. Nature Biotechnol. 2004; 22:70–7. [PubMed: 14647305]

17. Szymczak AL, Workman CJ, Wang Y, et al. Correction of multi-gene deficiency *in vivo* using a single 'self-cleaving' 2A peptide-based retroviral vector. Nature Biotechnol. 2004; 22:589–94. [PubMed: 15064769]
18. Lin K- Y, Guarnieri FG, Staveley-O'Carroll KF, et al. Treatment of established tumors with a novel vaccine that enhances major histocompatibility class II presentation of tumor antigen. Cancer Res. 1996; 56:21–6. [PubMed: 8548765]
19. Hung CF, Calizo R, Tsai YC, He L, Wu TC. A DNA vaccine encoding a single-chain trimer of HLA-A2 linked to human mesothelin peptide generates anti-tumor effects against human mesothelin-expressing tumors. Vaccine. 2007; 25:127–35. [PubMed: 16930783]
20. Chen CH, Wang TL, Hung CF, et al. Enhancement of DNA vaccine potency by linkage of antigen gene to an HSP70 gene. Cancer Res. 2000; 60:1035–42. [PubMed: 10706121]
21. Hung CF, Tsai YC, He L, Wu TC. Control of mesothelin-expressing ovarian cancer using adoptive transfer of mesothelin peptide-specific CD8+ T cells. Gene Ther. 2007; 14:921–9. [PubMed: 17377599]
22. Feltkamp MC, Smits HL, Vierboom MP, et al. Vaccination with cytotoxic T lymphocyte epitope-containing peptide protects against a tumor induced by human papillomavirus type 16-transformed cells. Eur J Immunol. 1993; 23:2242–9. [PubMed: 7690326]
23. Srivastava P. Interaction of heat shock proteins with peptides and antigen presenting cells: chaperoning of the innate and adaptive immune responses. Annu Rev Immunol. 2002; 20:395–425. [PubMed: 11861608]
24. Sanchez-Perez L, Kottke T, Daniels GA, et al. Killing of normal melanocytes, combined with heat shock protein 70 and CD40L expression, cures large established melanomas. J Immunol. 2006; 177:4168–77. [PubMed: 16951382]
25. Theriault JR, Mambula SS, Sawamura T, Stevenson MA, Calderwood SK. Extracellular Hsp70 binding to surface receptors present on antigen presenting cells and endothelial/epithelial cells. FEBS Lett. 2005; 579:1951–60. [PubMed: 15792802]
26. Whittall T, Wang Y, Younson J, et al. Interaction between the CCR5 chemokine receptors and microbial HSP70. Eur J Immunol. 2006; 36:2304–14. [PubMed: 16909434]
27. Wang Y, Kelly CG, Karttunen JT, et al. CD40 is a cellular receptor mediating mycobacterial heat shock protein 70 stimulation of CC-chemokines. Immunity. 2001; 15:971–83. [PubMed: 11754818]
28. Asea A, Rehli M, Kabingu E, et al. Novel signal transduction pathway utilized by extracellular HSP70: role of toll-like receptor (TLR) 2 and TLR4. J Biol Chem. 2002; 277:15028–34. [PubMed: 11836257]
29. Becker T, Hartl FU, Wieland F. CD40, an extracellular receptor for binding and uptake of Hsp70-peptide complexes. J Cell Biol. 2002; 158:1277–85. [PubMed: 12356871]
30. Noessner E, Gastpar R, Milani V, et al. Tumor-derived heat shock protein 70 peptide complexes are cross-presented by human dendritic cells. J Immunol. 2002; 169:5424–32. [PubMed: 12421917]
31. Li Z, Menoret A, Srivastava P. Roles of heat-shock proteins in antigen presentation and cross-presentation. Curr Opin Immunol. 2002; 14:45–51. [PubMed: 11790532]
32. Chen K, Lu J, Wang L, Gan YH. Mycobacterial heat shock protein 65 enhances antigen cross-presentation in dendritic cells independent of Toll-like receptor 4 signaling. J Leukoc Biol. 2004; 75:260–6. [PubMed: 14597728]
33. Flohe SB, Bruggemann J, Lendemans S, et al. Human heat shock protein 60 induces maturation of dendritic cells versus a Th1-promoting phenotype. J Immunol. 2003; 170:2340–8. [PubMed: 12594256]
34. Tseng JC, Hurtado A, Yee H, et al. Using Sindbis viral vectors for specific detection and suppression of advanced ovarian cancer in animal models. Cancer Res. 2004; 64:6684–92. [PubMed: 15374985]
35. Jenkins DE, Oei Y, Hornig YS, et al. Bioluminescent imaging (BLI) to improve and refine traditional murine models of tumor growth and metastasis. Clin Exp Metastasis. 2003; 20:733–44. [PubMed: 14713107]

36. Drake JM, Gabriel CL, Henry MD. Assessing tumor growth and distribution in a model of prostate cancer metastasis using bioluminescence imaging. Clin Exp Metastasis. 2005; 22:674–84. [PubMed: 16703413]

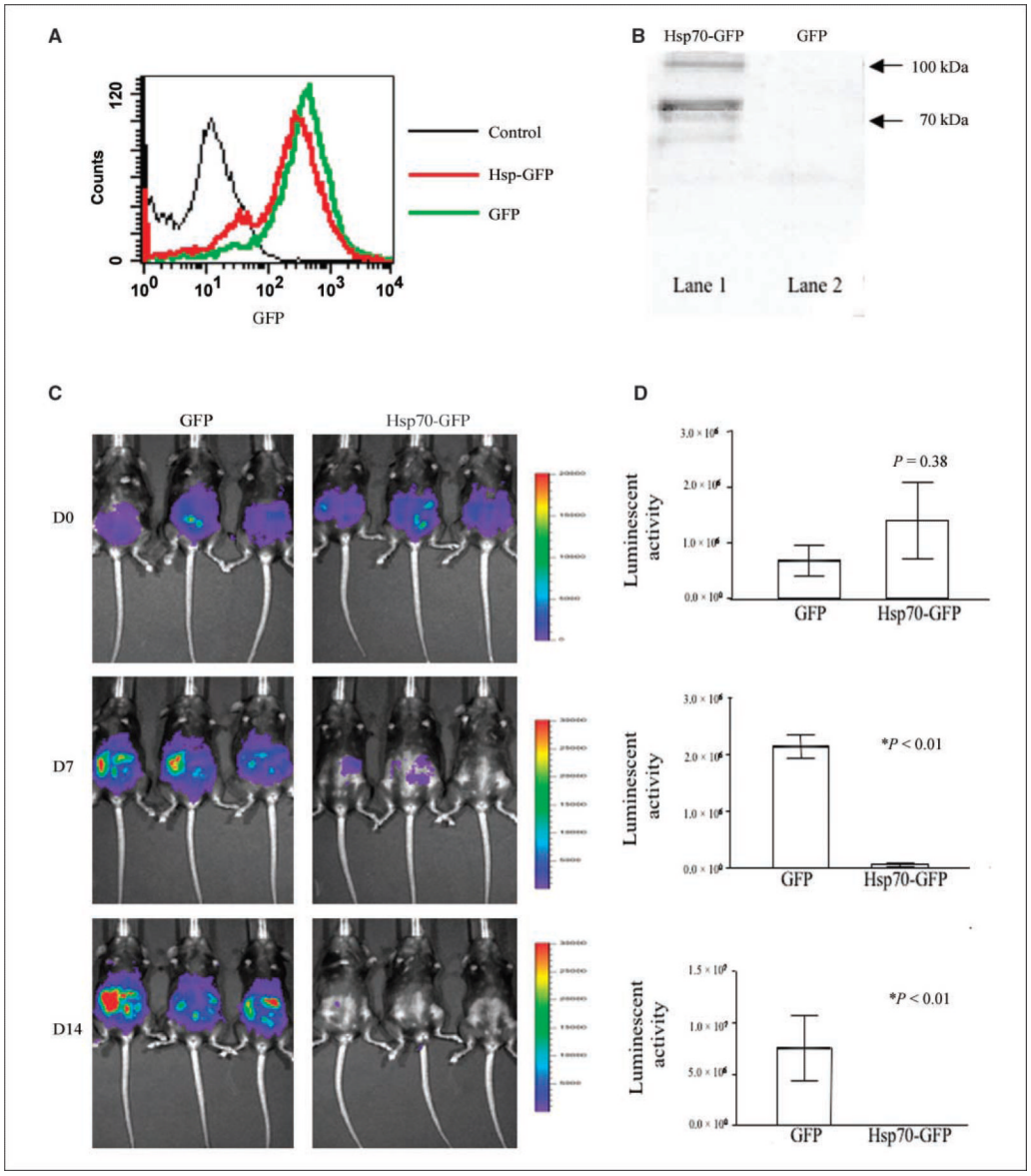

Figure 1.

In vivo tumor growth experiments in mice challenged with MOSEC/luc cells expressing either Hsp70-GFP or GFP following characterization of MOSEC/luc cell line transduced with sHsp70-T2A-GFP or T2A-GFP. *A*, flow cytometry analysis showing GFP expression level in MOSEC/luc cells transduced with retrovirus containing either sHsp70-T2A-GFP (*Hsp70-GFP*) or T2A-GFP (*GFP*). The untransfected cells were used as a control. *B*, Western blot analysis showing the expression of secreted mouse Hsp70 protein. The supernatant from the culture medium of luciferase-expressing MOSEC cells (MOSEC/luc) transfected with Hsp70-GFP (*lane 1*) or GFP (*lane 2*) was used for Western blot analysis using antibody specific to Hsp70. *Lane 1*, the higher molecular weight band (~100 kDa) represents the uncleaved fusion protein of sHsp70 and EGFP. *C*, luminescence images of representative C57BL/6 mice (five per group) challenged with MOSEC/luc cells expressing Hsp70-GFP or GFP on days 0 (*D0*), 7 (*D7*), and 14 (*D14*) after tumor challenge. *D*, quantification of luminescent activity in mice challenged with MOSEC/luc cells transfected with Hsp70-GFP or GFP on days 0, 7, and 14. *Columns*, mean; *bars*, SD. C57BL/6 mice

(five per group) were i.p. challenged with 1×10^6 per mouse of viable MOSEC/luc cells expressing either Hsp70-GFP or GFP. Tumor-challenged mice were imaged using the IVIS Imaging System Series 200. Bioluminescence signals were acquired for 1 min. The *P* values are included in the figure and the groups with statistical significance ($P < 0.05$) are indicated by asterisks.

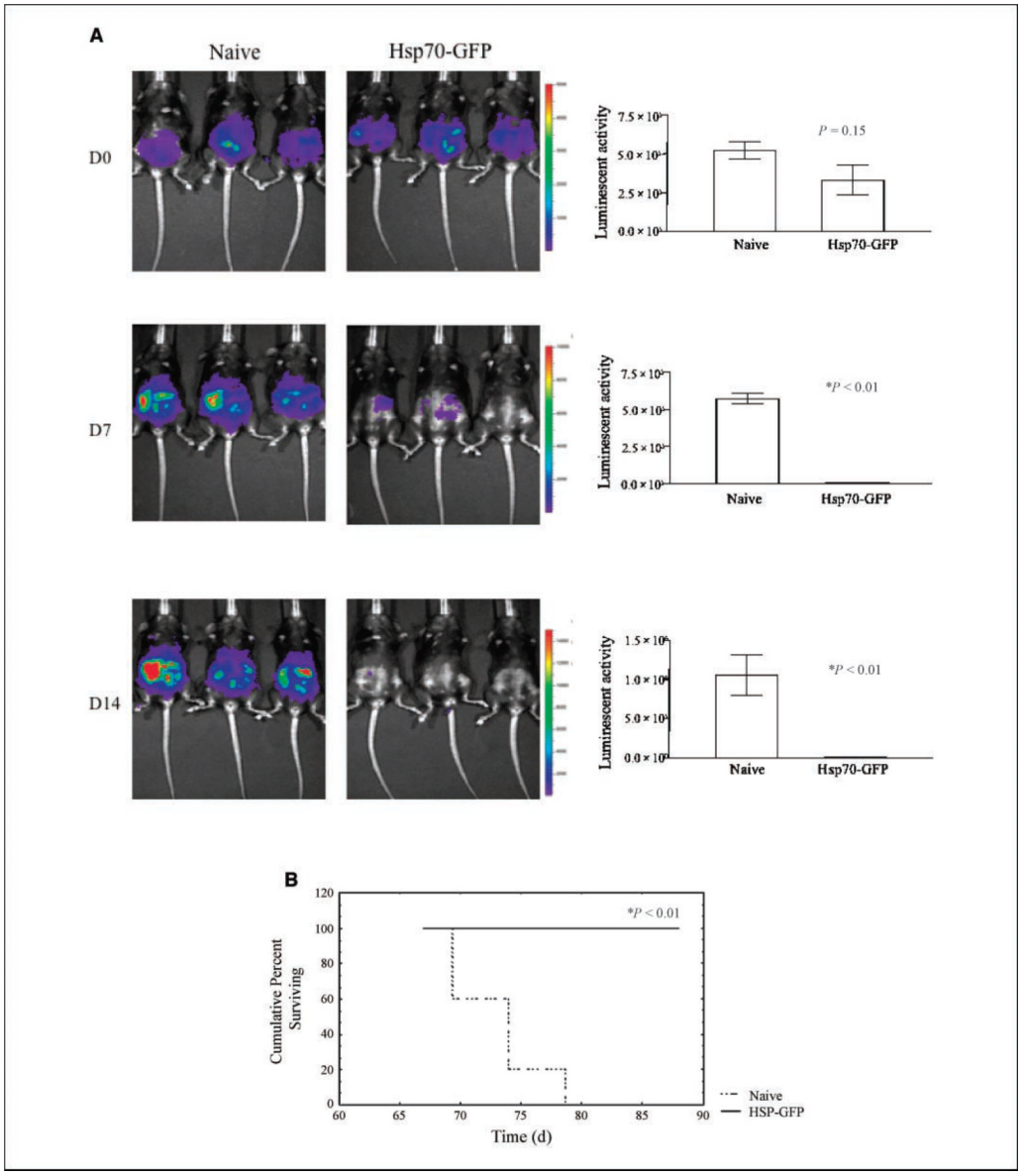

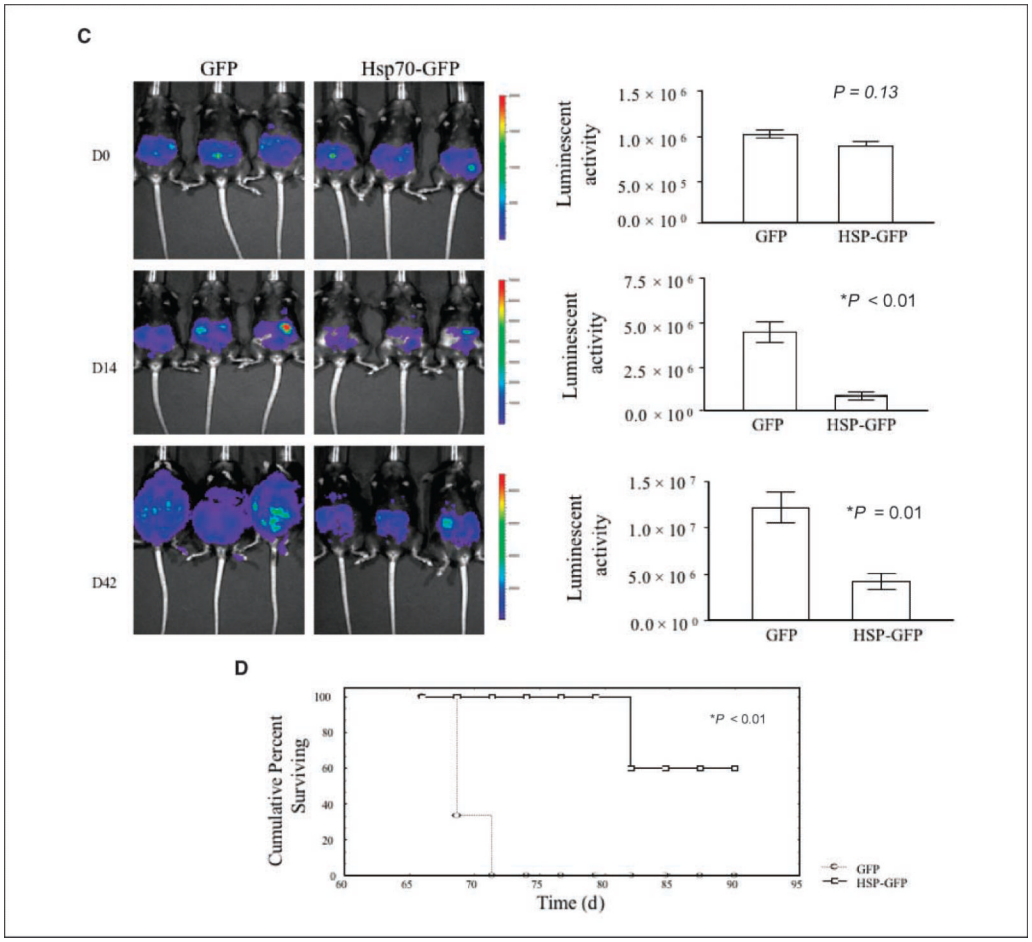

Figure 2.

In vivo tumor protection experiment in mice immunized i.p. with live or irradiated MOSEC/luc cells expressing Hsp70-GFP or GFP. C57BL/6 mice (five per group) that were previously challenged with MOSEC/luc expressing Hsp70-GFP were rechallenged i.p. after 2 wk with 1×10^6 per mouse of MOSEC/luc cells. As a control, a group of naive mice was challenged with 1×10^6 per mouse of live MOSEC/luc cells. Mice were imaged using the IVIS Imaging System Series 200. Bioluminescence signals were acquired for 1 min. *A*, representative luminescence images of naive mice challenged with MOSEC/luc cells and mice rechallenged with MOSEC/luc cells on days 0, 7, and 14. *Right*, quantification of luminescent activity in naive mice or mice rechallenged with MOSEC/luc cells on days 0, 7, and 14. *Columns*, mean; *bars*, SD. *B*, Kaplan-Meier survival analysis showing long-term survival in mice rechallenged with MOSEC/luc cells compared with naive mice control. C57BL/6 mice (five per group) were also immunized with 1×10^6 per mouse of irradiated MOSEC/luc cells expressing Hsp70-GFP or GFP. Two weeks after immunization, the vaccinated mice were challenged with 1×10^6 per mouse of MOSEC/luc cells. Mice were imaged using the IVIS Imaging System Series 200. Bioluminescence signals were acquired for 1 min. *C*, luminescence images of representative mice immunized with irradiated MOSEC/luc cells expressing Hsp70-GFP or GFP on days 0, 14, and 42. *Right*, quantification of luminescent activity in mice immunized with irradiated MOSEC/luc cells expressing Hsp70-GFP or GFP on days 0, 14, and 42. *Columns*, mean; *bars*, SD. *D*, Kaplan-Meier survival analysis showing long-term survival in mice immunized with MOSEC/luc cells expressing Hsp70-GFP compared with MOSEC/luc cells expressing GFP. The *P*

values are included in the figure and the groups with statistical significance ($P < 0.05$) are indicated by asterisks.

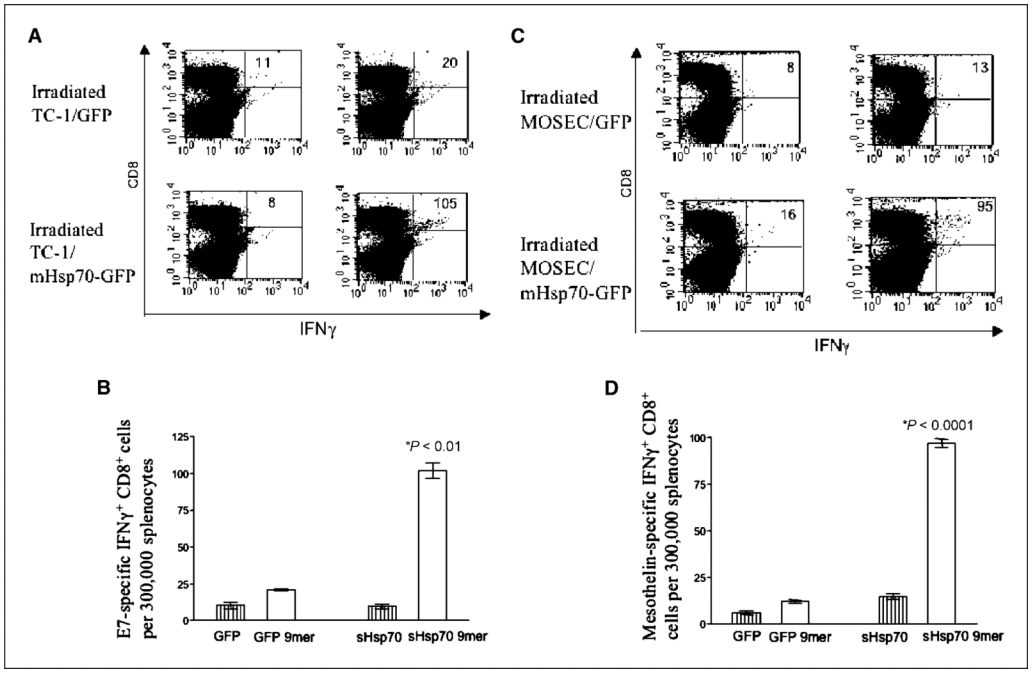

Figure 3.

Flow cytometry analysis of IFN-γ–secreting antigen-specific $CD8^+$ cell precursors in mice vaccinated with TC-1 or MOSEC cell-based vaccines. *A* and *B*, C57BL/6 mice (five per group) were vaccinated i.p. with 1×10^6 per mouse of irradiated TC-1/luc cells expressing either Hsp70-GFP or GFP twice with a 1-wk interval. *C* and *D*, C57BL/6 mice were vaccinated i.p. with 1×10^6 per mouse of irradiated MOSEC/luc cells expressing Hsp70-GFP or GFP twice with a 1-wk interval. Determination of the CD8 cells was done by culturing the splenocytes from vaccinated mice with E7 peptide (*A* and *B*) or mesothelin peptide (*C* and *D*) and analyzed for CD8 and intracellular IFN-γ staining by flow cytometry. *A*, representative flow cytometry data showing the number of E7-specific IFN-γ^+ $CD8^+$ T cells in the mice vaccinated with irradiated TC-1/luc cells expressing Hsp70-GFP or GFP. *B*, number of IFN-γ^+ $CD8^+$ T cells from each group with (*white columns*) or without (*shaded columns*) stimulation by the E7 peptide. *Columns*, mean; *bars*, SD. *C*, representative flow cytometry data showing the number of mesothelin-specific IFN-γ^+ $CD8^+$ T cells in mice vaccinated with irradiated MOSEC/luc cells expressing either Hsp70-GFP or GFP. *D*, number of mesothelin-specific IFN-γ^+ $CD8^+$ T cells from each group with (*white columns*) or without (*shaded columns*) stimulation by the mesothelin peptide. *Columns*, mean; *bars*, SD. The *P* values are included in the figure and the groups with statistical significance ($P < 0.05$) are indicated by asterisks.

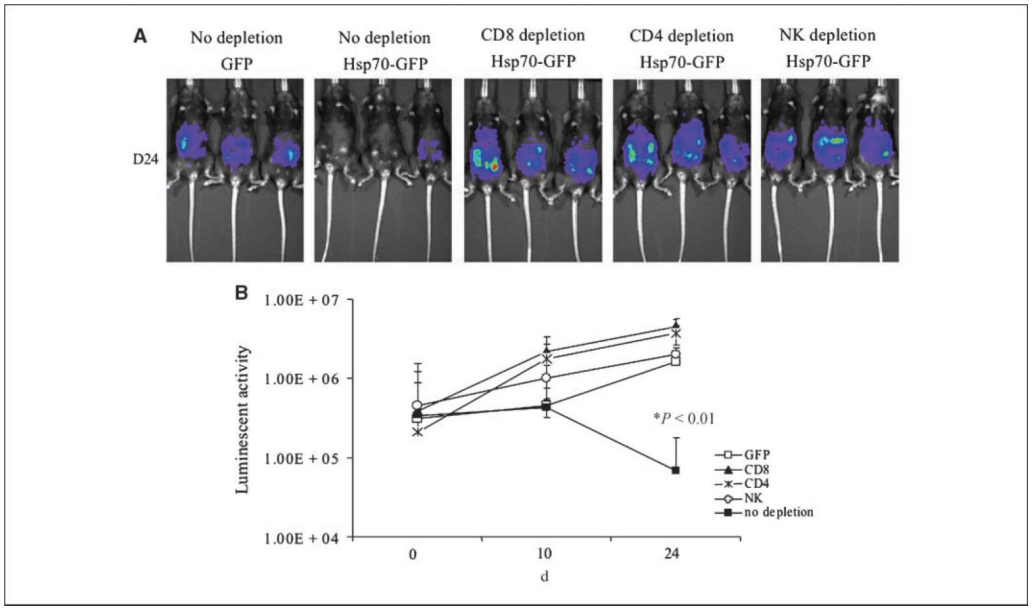

Figure 4.

In vivo antibody depletion experiment. C57BL/6 mice (five per group) were i.p. immunized with 1×10^6 per mouse of irradiated MOSEC/luc cells expressing Hsp70-GFP or GFP. Two weeks after vaccination, the immunized mice were challenged with 1×10^6 per mouse of MOSEC/luc cells. One week after the vaccination, the Hsp70-GFP–vaccinated mice were depleted of CD8, CD4, or NK cells using 100 μg each of purified rat mAbs 2.43, 100 GK1.5, and PK136, respectively. The mice were injected with antibodies every other day for three times for the first week and then once every week using a protocol similar to one described previously (20). Mice were imaged using the IVIS Imaging System Series 200. Bioluminescence signals were acquired for 1 min. *A*, luminescence images in representative mice challenged with MOSEC/luc cells expressing Hsp70-GFP with CD4 depletion, CD8 depletion, or NK depletion and MOSEC/luc cells expressing GFP. *B*, quantification of luminescent activity in the tumors of mice challenged with MOSEC/luc cells expressing Hsp70-GFP with CD4 depletion, CD8 depletion, or NK depletion and MOSEC/luc cells expressing GFP. The *P* values are included in the figure and the groups with statistical significance ($P < 0.05$) are indicated by asterisks.

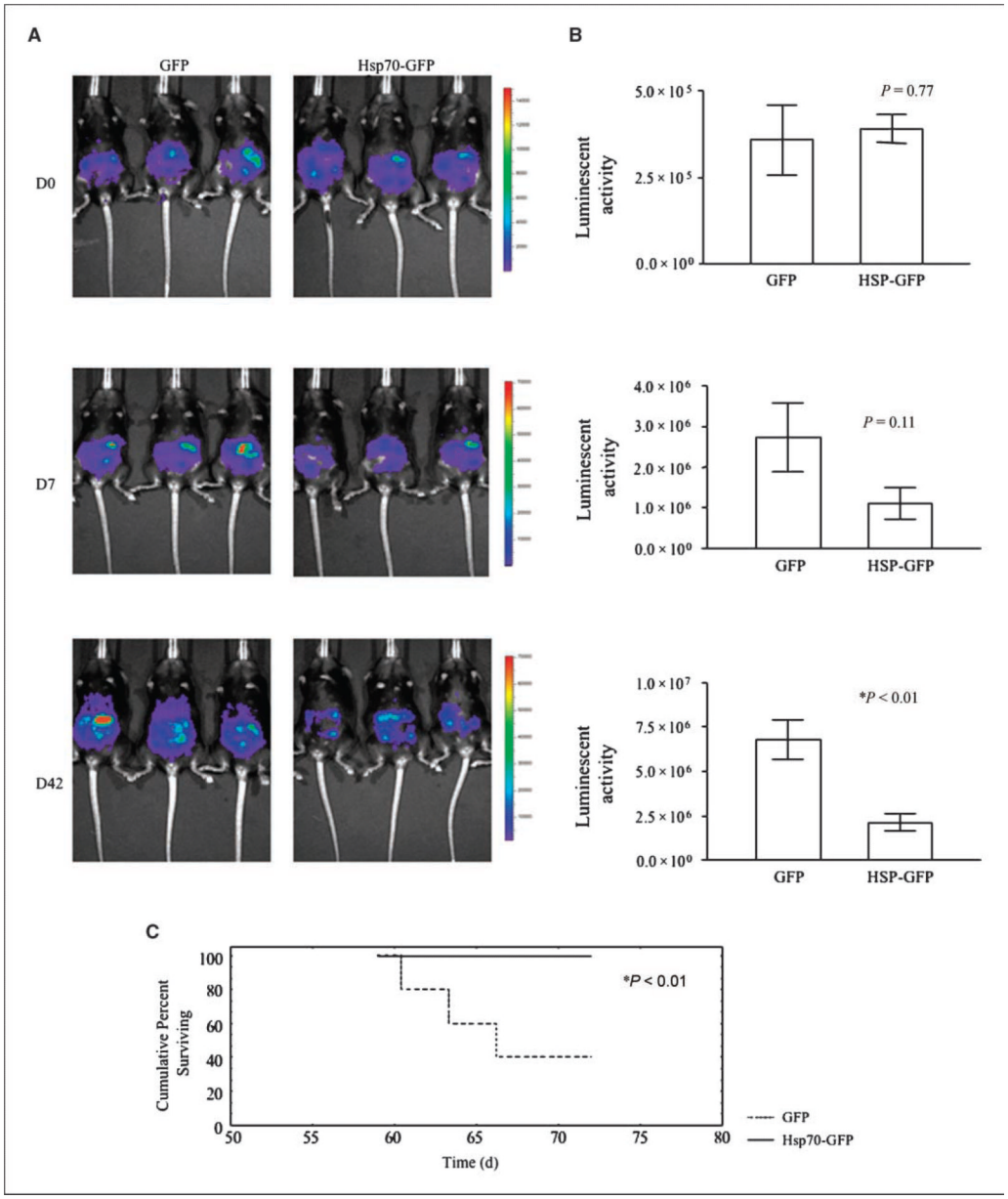

Figure 5.

In vivo tumor treatment. C57BL/6 mice (five per group) were i.p. challenged with 1×10^6 per mouse of MOSEC/luc cells. Five days later, the mice were treated with 1×10^6 per mouse of irradiated MOSEC/luc cells expressing either Hsp70-GFP or GFP. Mice were imaged using the IVIS Imaging System Series 200. Bioluminescence signals were acquired for 1 min. *A*, luminescence images in representative mice treated with MOSEC/luc cells expressing Hsp70-GFP or GFP on days 0, 7, and 42. *B*, quantification of luminescent activity in mice treated with MOSEC/luc cells expressing Hsp70-GFP or GFP on days 0, 7, and 42. *C*, Kaplan-Meier survival analysis showing long-term survival in mice treated with irradiated MOSEC/luc cells expressing Hsp70-GFP compared with the mice treated with the irradiated MOSEC/luc cells expressing GFP. The *P* values are included in the figure and the groups with statistical significance ($P < 0.05$) are indicated by asterisks.

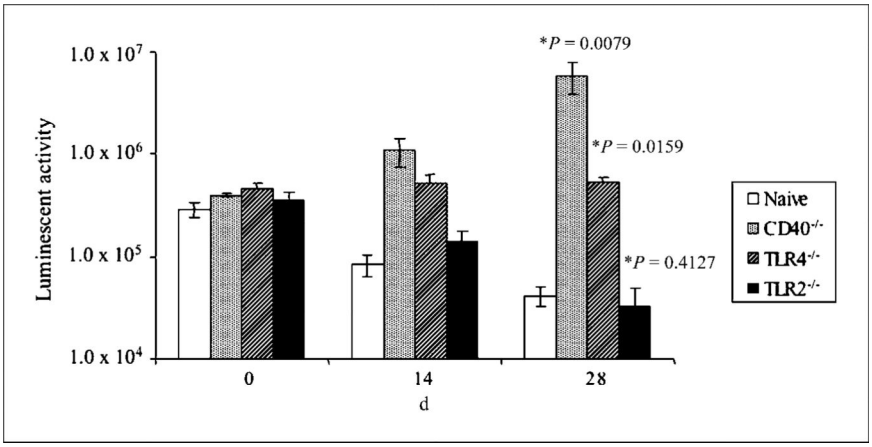

Figure 6.

In vivo tumor growth experiment in CD40, TLR2, and TLR4 knockout mice challenged with MOSEC/luc cells expressing Hsp70-GFP. Quantification of tumor load (luminescent activity) in CD40, TLR2, or TLR4 knockout C57BL/6 mice (five per group) challenged with viable MOSEC/luc cells expressing Hsp70-GFP on days 0, 14, and 28. Naive C57BL/6 mice challenged with MOSEC/luc cells expressing Hsp70-GFP were used as control. C57BL/6 mice (five per group) were i.p. challenged with 1×10^6 per mouse of the viable Hsp70-secreting tumor cells. Bioluminescence signals were acquired for 1 min. *Columns*, mean; *bars*, SD. The *P* values are included in the figure and the groups with statistical significance ($P < 0.05$) are indicated by asterisks.